Materials Research. 2026; 29: e20260113
DOI: https://doi.org/10.1590/1980-5373-MR-2026-0113

Influence of Discharge Energy on the Morphology and Optical Response of Tungsten Oxide Thin Films Deposited by Reactive High-Power Impulse Sputtering in a Facing-Target Configuration

Yoji Yasuda*[a]

[a]*Tokyo Polytechnic University, Faculty of Engineering, 5-45-1 Iiyama-minami, 243-0297, Atsugi, Kanagawa, Japan.*

Received: April 12, 2026; Revised: May 18, 2026; Accepted: July 02, 2026

Tungsten oxide thin films were deposited by reactive high-power impulse sputtering using a facing-target configuration (HiP-FTS), and the influence of discharge energy on film morphology and hydrogen response was investigated. The pulse width was varied at a constant repetition frequency to control the discharge energy delivered per pulse under identical gas flow conditions. An increase in pulse width enhanced the deposition rate and promoted smooth and compact surface morphologies, as indicated by SEM and AFM observations. Under fixed oxygen flow conditions, changes in film appearance and optical behavior suggested possible changes related to oxygen-deficient-like optical behavior at longer pulse widths. The hydrogen-induced optical response of Pt-loaded films was evaluated under 4% H_2 in Ar at room temperature. The films exhibited limited gasochromic response despite identical Pt loading conditions, indicating that hydrogen incorporation within the film structure may be limited by the compact microstructure formed under HiP-FTS conditions. These results indicate that discharge energy strongly influences film morphology, optical behavior, and hydrogen response in tungsten oxide thin films deposited by reactive high-power impulse sputtering with a facing-target configuration.

Keywords: *Tungsten oxide; High-power impulse magnetron sputtering; Facing-target sputtering; Reactive sputtering; Pulse width; Hydrogen gas sensing.*

1. Introduction

Hydrogen is attracting increasing attention as a clean and sustainable energy carrier; however, its wide flammability range and low ignition energy require reliable hydrogen detection technology. Among the various sensing approaches, optical and electrical hydrogen sensors based on metal oxide coatings have been extensively studied because of their chemical stability, durability, and compatibility with vacuum-based thin-film fabrication processes[1-3]. Tungsten oxide (WO_3) is one of the most promising oxide materials for hydrogen sensing owing to its reversible gasochromic behavior, in which hydrogen insertion leads to the formation of tungsten bronze (H_xWO_3) accompanied by a pronounced color change from transparent to deep blue [4-9]. Because of this distinct and reversible optical response, WO_3 has been widely studied for optical hydrogen sensors and smart window applications[7]. The gasochromic and sensing performance of WO_3 coatings strongly depends on their microstructure, stoichiometry, crystallinity, and defect concentration, particularly oxygen vacancies[10-12]. These structural features govern hydrogen dissociation, diffusion, and charge transfer processes, and thus determine the magnitude and reversibility of the optical response of the material. Consequently, extensive efforts have been devoted to tailoring WO_3 thin films by controlling deposition parameters, such as the oxygen partial pressure, substrate temperature, and post-deposition treatments[4,10,11].

Reactive magnetron sputtering is widely employed for depositing WO_3 coatings because of its scalability and compatibility with industrial coating technologies. However, conventional DC or RF sputtering often results in limited control over film morphology and defect structures, particularly under high deposition-rate conditions. High-Power Impulse Magnetron Sputtering (HiPIMS) has emerged as an advanced sputtering technique capable of generating highly ionized metal fluxes, enabling the growth of smooth thin films with improved adhesion[13-17]. These advantages make HiPIMS particularly attractive for functional oxide coatings. In reactive HiPIMS processes, the selection of pulse parameters plays a critical role in determining the discharge characteristics, ionization degree, and balance between the metal and reactive gas fluxes. It has been reported that reactive HiPIMS can modify hysteresis behavior depending on process conditions and material systems[18]. Furthermore, temporal pulse parameters, such as pulse width, duty cycle, and off-time, strongly influence the plasma dynamics, target oxidation behavior, and resulting film composition and optical behavior[17,19]. Experimental studies on oxide systems have demonstrated that inappropriate pulse conditions may lead to insufficient oxidation or excessively compact film structures, both of which can degrade the functional properties[20]. In the facing-target sputtering configuration, the closed magnetic field between the facing targets enhances plasma confinement and reduces the direct bombardment of the substrate by high-energy negative oxygen ions. This configuration enables the formation of smooth and compact films under relatively low substrate-damage conditions.

*e-mail: yyasuda@t-kougei.ac.jp
Associate Editor: Aloisio Klein.
Editor-in-Chief: Luiz Antonio Pessan.

Surface catalytic modification using noble metals such as platinum (Pt) is widely employed to enhance hydrogen dissociation and promote gasochromic responses in WO_3-based systems[7,11,12]. However, the formation of excessively compact microstructures in WO_3 films, while beneficial for mechanical robustness and smooth morphology, may suppress hydrogen transport within the films and insertion into the lattice structure. This finding suggests an intrinsic trade-off between structural stability and functional gasochromic activity. However, the interplay between discharge energy, oxidation behavior, and film morphology in reactive high-power impulse facing-target sputtering (HiP-FTS) has not yet been systematically clarified for WO_3 films. Therefore, this study aimed to establish correlations between discharge energy, morphological evolution, optical-property-related changes, and hydrogen-induced optical response in WO_3 thin films. Particular emphasis was placed on understanding how discharge-energy-dependent changes in film morphology influence hydrogen response behavior.

2. Experimental Methods

2.1. HiP-FTS system

WO_3 thin films were deposited using a High-Power Impulse Magnetron Sputtering (HiPIMS) system combined with a facing-target sputtering configuration originally designed and developed in our laboratory[21,22]. The system consisted of two tungsten targets (50 mm in diameter and 5 mm in thickness) mounted face-to-face with a target-to-target distance of 50 mm. An alkali-free glass substrate EAGLE XG (Corning Inc.) (40 mm × 30 mm × 0.7 mm) was positioned outside the direct plasma region, enabling a deposition environment essentially free from energetic negative ion bombardment. A HiPIMS pulsed power supply (HiPSTER1, IONAUTiCS) was used in combination with a DC power supply (MDX, Advanced Energy). A schematic of the HiP-FTS system and power supply connection is shown in Figure 1. Both facing tungsten targets were electrically connected to the same pulsed power supply and operated simultaneously during deposition.

2.2. Deposition conditions

Reactive sputtering was performed using an Ar/O_2 gas mixture. The base pressure prior to deposition was approximately 1.3×10^{-4} Pa, which was achieved using a combination of an oil diffusion pump and a rotary pump. Argon and oxygen gases were introduced into the chamber through mass flow controllers to precisely regulate the desired gas flow rates of 7 sccm for Ar (99.99% pure) and 4 sccm for O_2 (99.9% pure). W targets with a purity of 99.97% were used. The pulse width was varied from 10 to 80 ms while maintaining a constant repetition frequency of 800 Hz. The voltage pulse waveform was fixed at 800 V, and all depositions were performed at a working pressure of 1.3 Pa. The deposition time was adjusted for each pulse-width condition to obtain films with comparable thicknesses for optical and gasochromic evaluation. The resulting film thicknesses were 255, 278, 292, 285, and 260 nm for pulse widths of 10, 20, 40, 60, and 80 μs, respectively, corresponding to deposition times of 57.4, 19.8, 11.2, 9.0, and 5.1 min. To prevent thermal damage to the tungsten targets during high-power pulsed operation, the output power of the pulsed power supply was limited to 500 W. The oxygen flow rate was adjusted to form tungsten oxide films, and particular attention was paid to the time delay and persistence of the target oxidation following changes in the oxygen flow.

2.3. Characterization

The film thickness and deposition rate were evaluated using a stylus profilometer (Dektak3030, Sloan Technology). The surface morphology and roughness were examined using scanning electron microscopy (FE-SEM, S-5000, Hitachi High-Technologies) and atomic force microscopy (AFM, Nano ScopeIII, Veeco). The optical transmittance in the visible wavelength range was measured using a spectrometer (FilmTek system).

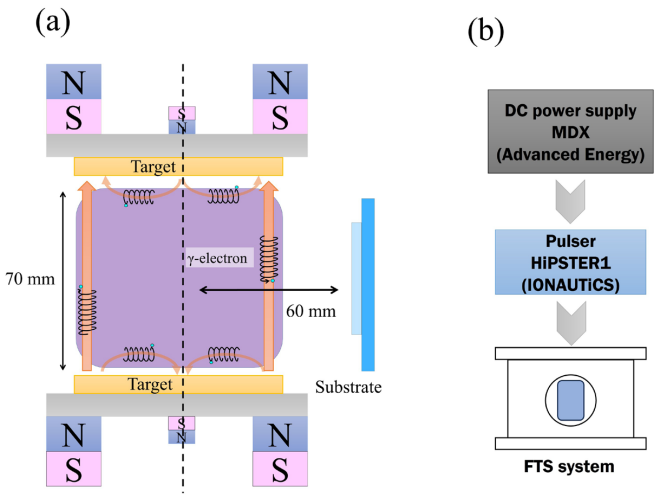

Figure 1. Schematic illustration of the High-Power Impulse Facing-Target Sputtering (HiP-FTS) system used in this study, including (a)* the arrangement of opposing tungsten targets, substrate position, and (b) power supply configuration. *Reprinted from Yasuda et al.[22].

The gasochromic properties were evaluated by exposing the films to a hydrogen-containing atmosphere (4% H_2 in Ar) at room temperature and observing the changes in their optical transmittance and visual appearance, as shown in Figure 2. Surface catalytic loading of Pt was carried out using an ion sputter coater (E-1030, Hitachi). Deposition was performed at a working pressure of 6 Pa with a sputtering current of 10 mA for 3 s. The short deposition time was selected to introduce a thin Pt overlayer to promote hydrogen dissociation at the film surface.

3. Results and Discussion

3.1. Discharge characteristics

Figure 3 shows the discharge current and target voltage waveforms for various pulse widths. A large discharge current region was obtained when the pulse width was 20 ms or less, which indicated efficient plasma generation. As the pulse width increased, the discharge duration was extended, leading to a higher total sputtered flux but also an increased sensitivity to target oxidation. It was also observed that the oxidation induced by the reactive oxygen gas persisted for a relatively long time after changes in the oxygen flow rate, requiring careful control of the process parameters. In HiPIMS discharges, it should be noted that the physical conditions at the cathode surface evolve dynamically during each HiPIMS pulse. In the early stage of the discharge, the plasma is primarily sustained by the working gas, whereas at later stages, sputtered metal species increasingly contribute to the discharge. Simultaneously, changes in cathode surface conditions, including local heating, oxidation state, and secondary electron emission behavior, may alter the discharge characteristics during the pulse. Such transient plasma–surface interactions are characteristic of HiPIMS processes and can influence the effective sputtering behavior under reactive conditions[23]. In the facing-target HiPIMS configuration, the plasma is strongly confined between the opposing cathodes, which enhances interactions between sputtered metal species and the discharge plasma. During each pulse, the discharge conditions may evolve dynamically from an Ar-dominated ignition stage to a metal-rich plasma state as sputtered tungsten accumulates in the confined plasma region, but this has not yet been clearly elucidated. A high peak current is directly associated with an increased ionization fraction of the sputtered metal species. The elongated pulse width in the present study increased the total energy delivered per pulse, thereby increasing both the time-integrated ion flux and the average discharge power. Although the repetition frequency was kept constant, a longer pulse-on time inevitably resulted in a higher discharge energy density. Under reactive conditions, this enhanced metal ion flux influences the oxidation kinetics at the growing surface. When the tungsten arrival rate exceeds the available oxygen supply under a fixed O_2 flow, oxygen-deficient-like film formation is likely to occur. Thus, the pulse width variation in the HiP-FTS system simultaneously modifies the plasma ionization characteristics and metal-to-oxygen flux balance.

3.2. Deposition rate and film appearance

Figure 4 shows the deposition rate and average discharge power as a function of pulse width. Both the deposition rate and the average discharge power increased monotonically with increasing pulse width under the fixed voltage (800 V) and repetition frequency (800 Hz) conditions. Increasing the pulse width extended the pulse-on time, resulting in a larger time-integrated discharge current and consequently higher average discharge power. The increased average discharge power enhanced the total sputtered flux, leading to a higher deposition rate. Under the fixed oxygen flow condition, this increase in sputtered tungsten flux is expected to have influenced the effective balance between sputtered metal species and supplied oxygen, resulting in pulse-width-dependent changes in film appearance and optical behavior.

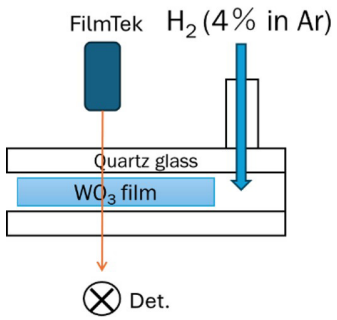

Figure 2. Schematic diagram of the optical transmittance measurement system used to evaluate the gasochromic response to hydrogen exposure.

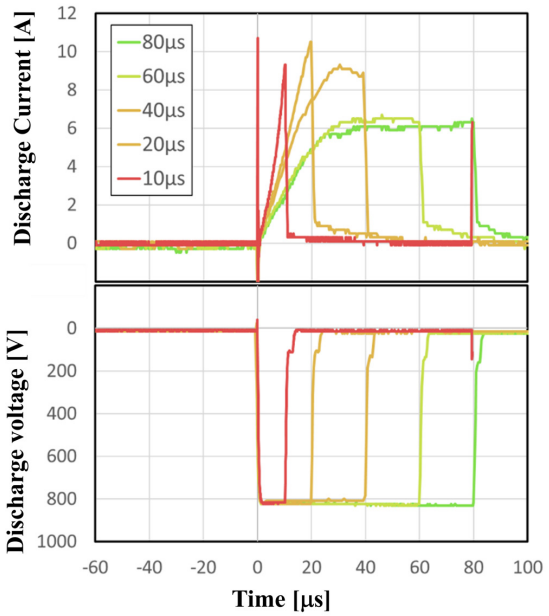

Figure 3. Typical discharge waveforms of target voltage and target current for different pulse widths (10–80 ms) under reactive Ar/O_2 sputtering conditions.

In HiPIMS plasmas, ionized metal species can return to the target (self-sputtering) or contribute to the sustained discharge current, further increasing the sputtering yield. Photographs of the as-deposited WO_3 films prepared at different pulse widths are shown in Figure 5. At pulse widths of 10 and 20 µs, the films appeared nearly colorless and transparent, indicating relatively sufficient oxidation under the present oxygen flow conditions. As the pulse width increased to 40 and 60 µs, the films gradually changed from pale yellow to greenish.

At the longest pulse width of 80 µs, the film exhibited a pronounced blue coloration that was clearly distinct from the weaker color variations observed at shorter pulse widths. This behavior suggests increased defect-related optical absorption under insufficient oxidation conditions. Such behavior is consistent with oxygen-deficient-like optical characteristics reported for tungsten oxide systems, although direct compositional or chemical-state confirmation was not performed in the present study. In addition, slight differences in film thickness and refractive index could also contribute to the observed color variations through thin-film interference effects. Therefore, the weaker color variations observed for the 10–60 µs samples should not be attributed solely to compositional changes.

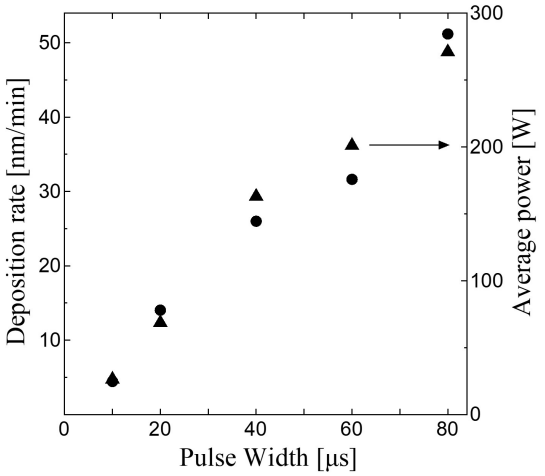

Figure 4. Dependence of deposition rate and average power on pulse width for WO_3 thin films deposited by HiP-FTS.

3.3. Surface morphology and roughness

Combined SEM–AFM analysis revealed that all films deposited at different pulse widths exhibited smooth and featureless surfaces and uniformly low surface roughness (Figure 6). The surface roughness Ra ranged from approximately 0.4 nm (10 ms) to 1.5 nm (60 ms), with no significant roughening even at longer pulse widths.

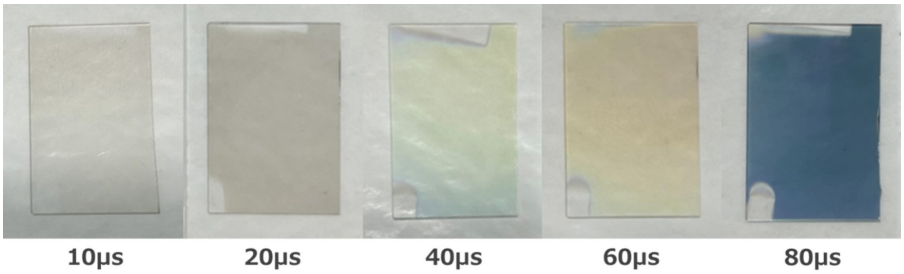

Figure 5. Photographs of as-deposited WO_3 thin films deposited at different pulse widths of 10, 20, 40, 60, and 80 ms under identical reactive sputtering conditions.

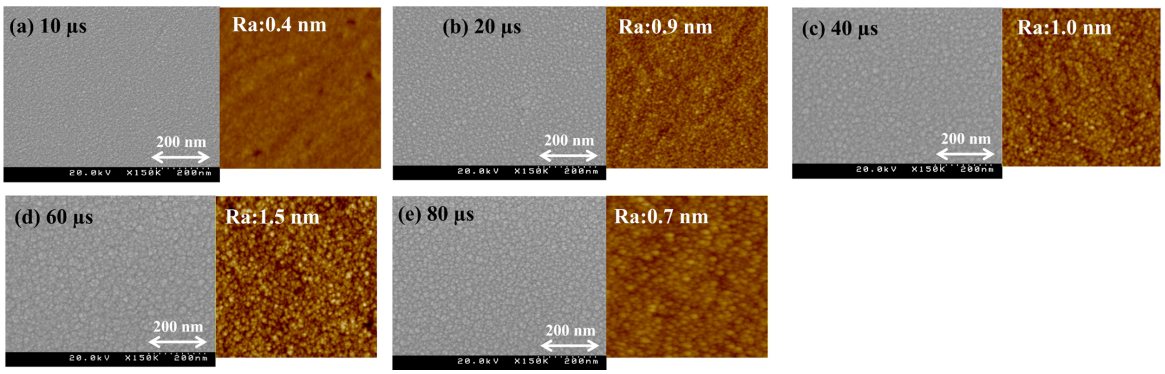

Figure 6. Combined SEM and AFM surface morphologies of WO_3 thin films deposited at different pulse widths. (a–e) SEM images and (a-e) corresponding AFM images showing smooth surfaces with low roughness.

This suggests that the HiP-FTS configuration effectively suppresses columnar growth and promotes the formation of smooth and compact surface morphologies. The smooth and featureless morphology observed across all pulse widths suggests that ion-assisted growth dominates shadowing-driven columnar growth. The high ion-to-neutral flux ratio characteristic of HiPIMS enhances surface diffusion and atomic rearrangement, leading to compact microstructures, even without substrate heating. Such smooth and compact morphologies are considered advantageous for mechanical stability; they may reduce the number of diffusion pathways required for hydrogen insertion.

3.4. Optical transmittance and gasochromic response

Figure 7 schematically illustrates the gasochromic mechanism of Pt-loaded WO_3 films and an example of their optical responses to hydrogen exposure. As shown in Figure 7, hydrogen molecules were dissociatively adsorbed on the Pt catalyst and subsequently inserted into the WO_3 lattice, leading to the formation of tungsten bronze (H_xWO_3), which is responsible for the blue color[19,20]. However, in the present study, the gasochromic response remained limited, suggesting that hydrogen transport within the film structure contribute to the limited response behavior. The limited gasochromic response observed in our HiP-FTS films is attributed, at least in part, to the limited presence of interconnected diffusion pathways such as pores or grain boundaries. In tungsten oxide, these structural features typically act as fast diffusion paths for hydrogen ions (H^+).

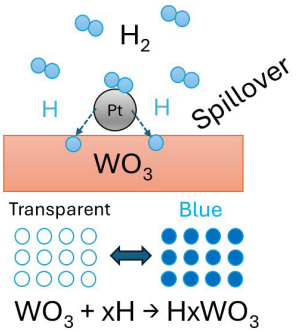

Figure 7. Schematic of the gasochromic mechanism in Pt-loaded WO_3, showing hydrogen insertion and tungsten bronze (H_xWO_3) formation.

The dense and compact films formed via HiP-FTS may reduce effective hydrogen transport within the bulk of the film, thereby constraining the coloration kinetics despite the presence of the Pt catalytic layer.

Figure 8 shows the optical transmittance spectra of the WO_3 thin films deposited at different pulse widths before and after exposure to hydrogen. Prior to hydrogen exposure, all films exhibited high optical transparency in the visible region, with only a moderate decrease in transmittance of approximately 10% above 500 nm, regardless of the pulse width. This result indicates that variations in pulse width had a limited influence on the optical transparency of the as-deposited films under the present conditions. Gasochromic coloration in WO_3 is associated with the formation of tungsten bronze (H_xWO_3), where hydrogen insertion leads to the partial reduction of W^{6+} to W^{5+} states. The resulting small polaron absorption typically increases optical absorption in the visible and near-infrared regions. In the present films, the limited optical response suggests that the hydrogen diffusion into the bulk WO_3 lattice was restricted. Since Pt loading was identical for all samples, surface catalytic dissociation of hydrogen is unlikely to be the dominant limiting factor[2,24]. Pt was deposited under identical conditions for all samples to minimize variations in catalytic loading, although its distribution may be influenced by surface morphology. Instead, the dense microstructure formed under HiP-FTS conditions likely suppresses bulk proton transport. This interpretation is consistent with the observed smooth morphology and low surface roughness of the films. To further examine the optical behavior of the deposited WO_3 films, the optical bandgap was estimated using the Tauc relation, $(\alpha h\nu)^n = A(h\nu - E_g)$, where α is the absorption coefficient, $h\nu$ is the photon energy, A is a proportionality constant, and E_g is the optical bandgap. Since WO_3 exhibits indirect optical transitions, an exponent of $n = 1/2$ was adopted, and E_g was determined from the linear extrapolation of $(\alpha h\nu)^{\frac{1}{2}}$ plotted as a function of photon energy to the horizontal axis (Figure 9)[25-27]. The estimated optical bandgap values were 3.10, 3.05, 3.05, 3.05, and 2.87 eV for films deposited at pulse widths of 10, 20, 40, 60, and 80 µs, respectively. Only modest variations in optical bandgap were observed among the 10–60 µs samples, whereas the 80 µs sample exhibited a more pronounced decrease. This trend is consistent with the distinct blue coloration observed for the 80 µs film and suggest increased defect-related optical absorption under longer pulse conditions.

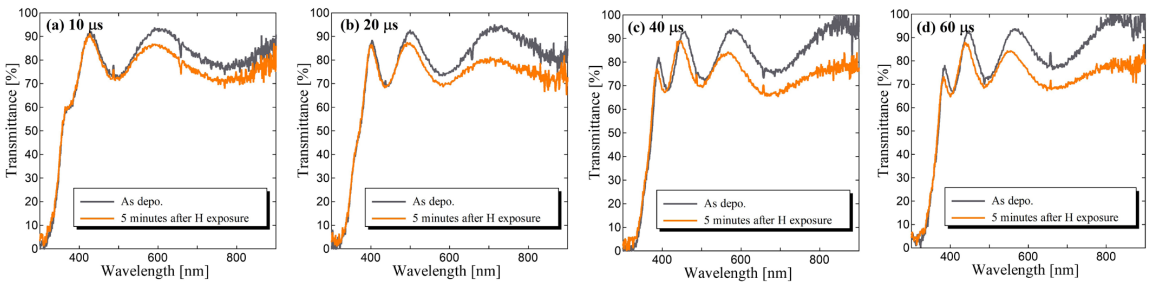

Figure 8. Optical transmittance spectra of WO_3 thin films deposited at different pulse widths measured before and after exposure to 4% H_2 in Ar.

However, because direct compositional or chemical-state analyses were not performed in the present study, these optical changes should be interpreted cautiously. In addition, slight variations in film thickness and refractive index cannot be excluded as a contributing factor to the observed optical differences through thin-film interference effects. Therefore, although HiP-FTS enables mechanically stable coatings with smooth and compact morphologies, such compact microstructures are likely to compromise the functional gasochromic activity.

The gasochromic properties were evaluated by exposing the films to a hydrogen-containing atmosphere (4% H_2 in Ar) at room temperature, which was selected to simulate realistic operating conditions for practical hydrogen sensing applications.[28] However, no significant or reversible change in optical transmittance was observed for any of the films after hydrogen exposure, indicating weak gasochromic responses, as shown in Figure 10. Although the WO_3 films were surface-loaded with Pt to promote the dissociative adsorption of hydrogen, the gasochromic response remained weak. This result suggests that hydrogen insertion into the WO_3 lattice was kinetically limited, most likely because of the dense microstructure and limited defect-related transport pathways of the WO_3 films deposited by the HiP-FTS process, rather than insufficient surface catalytic activity. The present results suggest a trade-off inherent to the HiP-FTS deposition of WO_3 films. Increasing the discharge energy promotes the formation of smooth and compact surface morphologies, which are beneficial for mechanical durability and optical uniformity. However, the formation of compact morphologies is expected to reduce accessible diffusion pathways and defect-mediated transport channels necessary for efficient hydrogen insertion. Thus, optimization of WO_3-based hydrogen-sensing coatings requires balancing discharge energy, oxygen supply, and defect engineering. Pulse-width-controlled HiPIMS provides a powerful processing parameter for tuning this balance. These findings indicate that Pt loading alone is insufficient to achieve a strong gasochromic response when hydrogen insertion is limited by bulk transport processes. Therefore, further enhancement of the gasochromic and sensing performance requires deliberate control of the film density and defect structure, such as controlled modification of defect-related structures, controlled nanoporosity, or multilayer architectures, while maintaining the benefits of HiP-FTS deposition. From a processing perspective, pulse-width-controlled HiPIMS provides a promising route to tuning the balance between film compactness and functional performance. Optimization of pulse parameters in combination with Pt loading is expected to enable the fabrication of WO_3-based coatings that simultaneously exhibit mechanical robustness and enhanced hydrogen sensitivity. It should be noted that the compactness of the film microstructure and possible stoichiometry changes were inferred indirectly from deposition behavior and optical properties.

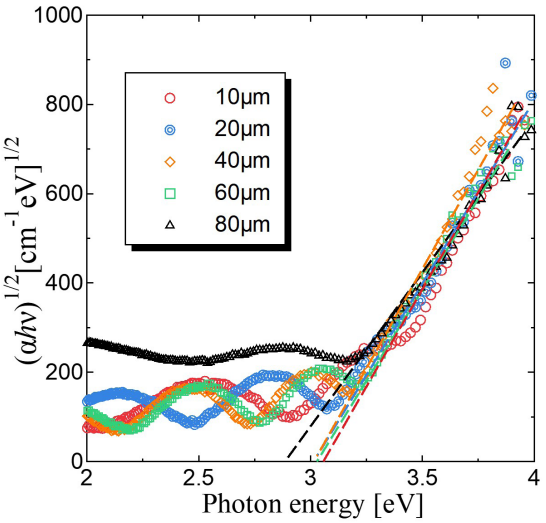

Figure 9. Tauc plots of WO_3 thin films deposited at pulse widths of 10, 20, 40, 60, and 80 μs, assuming an indirect optical transition.

4. Conclusions

Tungsten oxide thin films were deposited by reactive high-power impulse sputtering using a facing-target configuration, and the influence of pulse width on deposition behavior, film morphology, optical properties, and hydrogen response was investigated. Increasing pulse width increased both the average discharge power and deposition rate under fixed voltage and repetition frequency conditions, indicating that discharge energy strongly affects the deposition process. All films exhibited smooth surface morphologies with low roughness, while distinct pulse-width-dependent differences were observed in film appearance and optical behavior. Optical bandgap analysis based on Tauc plots showed only modest variations for films deposited at pulse widths between 10 and 60 μs, whereas the 80 μs sample exhibited a more pronounced decrease in bandgap to 2.87 eV, consistent with its distinct blue coloration. This optical trend may suggest increased defect-related absorption under longer pulse conditions, although direct compositional confirmation was

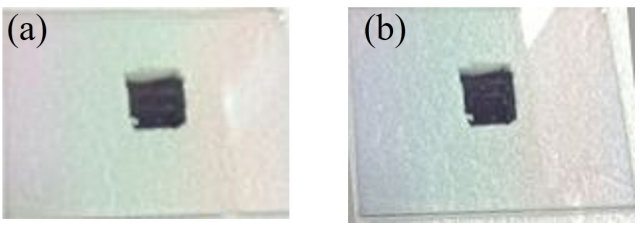

Figure 10. Photographs of WO_3 thin films (a) before and (b) after exposure to 4% H_2 in Ar, demonstrating a weak gasochromic response.

not performed. The Pt-loaded films exhibited only limited gasochromic response under 4% hydrogen exposure at room temperature. This result suggests that the compact film structures formed under the present deposition conditions may limit hydrogen incorporation into the WO_3 films. These results indicate that discharge energy is an important parameter governing the balance between film structure and functional gasochromic behavior in tungsten oxide thin films deposited by reactive high-power impulse sputtering with a facing-target configuration.

5. Data Availability

The entire dataset supporting the results of this study was published in the article itself.

6. References

1. Gao C, Guo X, Nie L, Wu X, Peng L, Chen J. A review on WO3 gasochromic film: Mechanism, preparation and properties. Int J Hydrogen Energy. 2023;48(6):2442.
2. Mirzaei A, Kim J-H, Kim HW, Kim SS. Gasochromic WO3 nanostructures for the detection of hydrogen gas: an overview. Appl Sci. 2019;9(9):1775.
3. Mazur M, Kapuścik P, Weichbrodt W, Domaradzki J, Mazur P, Kot M, et al. WO3 thin-film optical gas sensors based on gasochromic effect towards low hydrogen concentrations. Materials. 2023;16(10):3831.
4. Hsu W-C, Chan C-C, Peng C-H, Chang C-C. Hydrogen sensing characteristics of an electrodeposited WO3 thin film gasochromic sensor activated by Pt catalyst. Thin Solid Films. 2007;516(2–4):407.
5. Takahashi H, Okazaki S, Nishijima Y, Arakawa T. Optimization of hydrogen sensing performance of Pt/WO3 gasochromic film fabricated by the Sol-Gel method. Sens Mater. 2017;29:1259.
6. Wang L, Yu P, Yang K, Liu H, Yu A, Liu X, et al. Fast-response and highly reversible WO3/Pt gasochromic nanorod for eye-readable hydrogen leak detection at room temperature. Int J Hydrogen Energy. 2025;191:152240.
7. Granqvist CG. Electrochromics for smart windows: Oxide-based thin films and devices. Thin Solid Films. 2014;564:1.
8. Deb SK. A novel electrophotographic system. Appl Opt. 1969;8(S1):192.
9. Hübert T, Boon-Brett L, Black G, Banach U. Hydrogen sensors – A review. Sens Actuators B Chem. 2011;157(2):329.
10. Girão AF, Completo A. Eye-readable sensors for intuitive hydrogen monitoring. Int J Hydrogen Energy. 2024;65:593.
11. Ahmad MZ, Sadek AZ, Yaacob MH, Anderson DP, Matthews G, Golovko VB, et al. Optical characterisation of nanostructured Au/WO3 thin films for sensing hydrogen at low concentrations. Sens Actuators B Chem. 2013;179:125.
12. Kalanur SS, Yoo I-H, Lee Y-A, Seo H. Green deposition of Pd nanoparticles on WO3 for optical, electronic and gasochromic hydrogen sensing applications. Sens Actuators B Chem. 2015;221:411.
13. Anders A. Discharge physics of high power impulse magnetron sputtering. Surf Coat Tech. 2011;205(Suppl 2):S1.
14. Gudmundsson JT, Brenning N, Lundin D, Helmersson U. High power impulse magnetron sputtering discharge. J Vac Sci Technol A Vacuum, Surfaces Film. 2012;30(3):30801.
15. Sarakinos K, Alami J, Konstantinidis S. High power pulsed magnetron sputtering: A review on scientific and engineering state of the art. Surf Coat Tech. 2010;204(11):1661-84.
16. Samuelsson M, Lundin D, Jensen J, Raadu MA, Gudmundsson JT, Helmersson U. On the film density using high power impulse magnetron sputtering. Surf Coat Tech. 2010;205(2):591.
17. Anders A. Tutorial: reactive high power impulse magnetron sputtering (R-HiPIMS). J Appl Phys. 2017;121(17)
18. Wallin E, Helmersson U. Hysteresis-free reactive high power impulse magnetron sputtering. Thin Solid Films. 2008;516(18):6398.
19. Zhao X, Jin J, Cheng J-C, Lee J-W, Wu K-H, Liu K-C. Effect of pulsed off-times on the reactive HiPIMS preparation of zirconia thin films. Vacuum. 2015;118:38.
20. Nouvellon C, Michiels M, Dauchot JP, Archambeau C, Laffineur F, Silberberg E, et al. Deposition of titanium oxide films by reactive High Power Impulse Magnetron Sputtering (HiPIMS): influence of the peak current value on the transition from metallic to poisoned regimes. Surf Coat Tech. 2012;206(16):3542.
21. Naoe M, Hoshi Y, Yamanaka S. High rate deposition of magnetic films by sputtering from two facing targets. J Cryst Growth. 1978;45:361.
22. Yasuda Y, Yamada Y, Koshiji F, Kobayashi S, Uchida T, Hoshi Y. Effect of annealing treatment of indium tin oxide thin films on film properties and transparent antenna properties. Thin Solid Films. 2024;794:140295.
23. Hippler R, Cada M, Mutzke A, Hubicka Z. Pulse length dependence of a reactive high power impulse magnetron (HiPIMS) discharge. Plasma Sources Sci Technol. 2023;32(5):055013.
24. Liu H, Yang Z, Wang L, Yu P, Kang Z, Wu Q, et al. Gasochromic hydrogen sensors: fundamentals, recent advances, and perspectives. Sens Mater. 2023;35(1):39.
25. Tauc J, Grigorovici R, Vancu A. Optical properties and electronic structure of amorphous germanium. Phys Status Solidi. 1966;15(2):627.
26. Castro-Hurtado I, Tavera T, Yurrita P, Pérez N, Rodriguez A, Mandayo GG, et al. Structural and optical properties of WO 3 sputtered thin films nanostructured by laser interference lithography. Appl Surf Sci. 2013;276:229.
27. Hrubantova A, Hippler R, Wulff H, Cada M, Olejnicek J, Nepomniashchaia N, et al. Deposition of tungsten oxide films by reactive magnetron sputtering on different substrates. J Vac Sci Technol A. 2022;40(6)
28. Nishizawa K, Yamada Y, Yoshimura K. Low-temperature chemical fabrication of WO3 gasochromic switchable films: a comparative study of Pd and Pt nanoparticles dispersed WO3 films based on their structural and chemical properties. Thin Solid Films. 2020;709:138201.